New Insights into the Atomic-Scale Structures and Behavior of Steels

E. A. Marquis,[1] * P.-Pa Choi,[2] F. Danoix,[3] K. Kruska,[4] S. Lozano-Perez,[4] D. Ponge,[2] D. Raabe,[2] and C. A. Williams[4]

[1] Department of Materials Science and Engineering, University of Michigan, Ann Arbor, 48109 MI

[2] Max-Planck-Institut für Eisenforschung, Max-Planck-Str. 1, 40237 Düsseldorf, Germany

[3] Université de Rouen, UMR 6634 CNRS, Groupe de Physique des Materiaux, 76801 Saint Etienne du Rouvray, France

[4] Department of Materials, University of Oxford, Oxford, UK

* emarq@umich.edu

Introduction

Atom probe tomography (APT) has significantly contributed to our understanding and development of structural materials through the detailed analysis of solute behavior, cluster formation, precipitate evolution, and interfacial and grain boundary chemistry. Whether one is concerned with light alloys, Ni-based superalloys, or steels, the design objectives are similar: developing alloys with optimum properties (strength, toughness, ductility, fatigue resistance, creep strength) through controlled precipitation, grain structure, solute state, and combination of phases. Performance in service, through microstructural stability and resistance to degradation, is also a major design criterion for the development of novel materials.

The ability to probe the atomic-scale structure of complex structural alloys has been instrumental in providing key insights into the atomistic mechanisms controlling microstructure, in providing routes for the development of better alloys and in suggesting solutions to remediate problematic degradation phenomena. This article purposely focuses on the impact that APT has had on our understanding of steels, from the development of new strengthening strategies to designing materials more resistant to degradation. The chosen examples illustrate the power of APT in atom-by-atom analysis, three-dimensional reconstruction, and equal sensitivity for all chemical species, including light elements, such as carbon and nitrogen. Although this article shows results for steels, the applications illustrated are common to most metals systems studied, such as aluminum-based alloys, nickel-based alloys, and magnesium alloys.

TRIP Steels

Most advanced high-strength steels are currently designed via two main mechanisms. The transformation-induced plasticity (TRIP) and twinning-induced plasticity (TWIP) effects involve athermal deformation-induced transformations, such as martensite formation or twinning of unstable austenite during deformation [1]. Alternatively, nanoscale precipitation is used in maraging steels through thermal aging of martensite [2]. Other strengthening strategies are based on bainite formation and shear banding.

Athermal transformation and precipitation have been recently combined in a novel class of materials referred to as maraging-TRIP steels that were designed for superior strain hardening behavior [2]. These steels are precipitation-hardened austenitic-martensitic TRIP steels, combining both high strength with yield strengths up to 1.5 GPa and significant ductility (up to 20%) as shown in Figure 1. The alloys have low carbon concentrations (0.01 wt.% C), between 9 and 15 wt.% Mn depending on the desired volume fraction and stability of retained austenite, and minor additions of Ni, Al, Ti, and/or Mo (1–2 wt.%) [2] that are used to promote nanoscale precipitation in martensite during aging. The alloys are homogenized in the austenitic region and quenched. Depending on the Mn and Ni contents, the resulting microstructure is either fully martensitic (conventional maraging steels [1]) or martensitic with some amount of retained austenite (maraging-TRIP steels). After quenching, the material is heat-treated at a temperature that is 100–150 K below the bulk re-austenitization temperature (maraging treatment) to trigger the precipitation processes in the martensite (usually at 450°C), as revealed by APT, Figure 1. The APT analysis of interfaces between retained austenite and martensite also revealed that pronounced austenite reversion can take place during aging (for example, at 450°C, 48 h for the specimen shown in Figure 1), that is, far below the temperature for bulk re-transformation to austenite [2]. The Mn partitioning, in particular, at the martensite/austenite interface leads to the formation and growth of a new austenite layer on the existing retained austenite with drastically different composition compared to the bulk.

It is worth noting that the occurrence of two types of austenite with different stabilities (retained or reverted) leads to a broader deformation regime where the TRIP effect occurs. This mechanism appears to promote ductility. This example of Fe-Mn maraging TRIP steels illustrates how the combination of the two strengthening mechanisms opens a novel path to the development of ultrahigh-strength lean steels [2].

Precipitation Strengthening

Focusing on precipitation strengthening, carbon and nitrogen are common elements used for carbide and nitride formation. Comparing their behavior is instrumental in illustrating how precipitation pathways (homogeneous vs. heterogeneous) and resulting morphology and interface nature (coherent vs. semi-coherent vs. incoherent) of the precipitate phases are key elements to control their strengthening effectiveness. Figure 2a shows a 3D reconstruction obtained after analysis of a model low-alloyed ferritic FeNbC steel aged at 650°C. As clearly evidenced, niobium carbides have precipitated in specific locations, and precipitation occurs mostly heterogeneously on dislocations as revealed by previous TEM observations [3]. Although it was not possible to determine whether some homogeneous precipitation was occurring
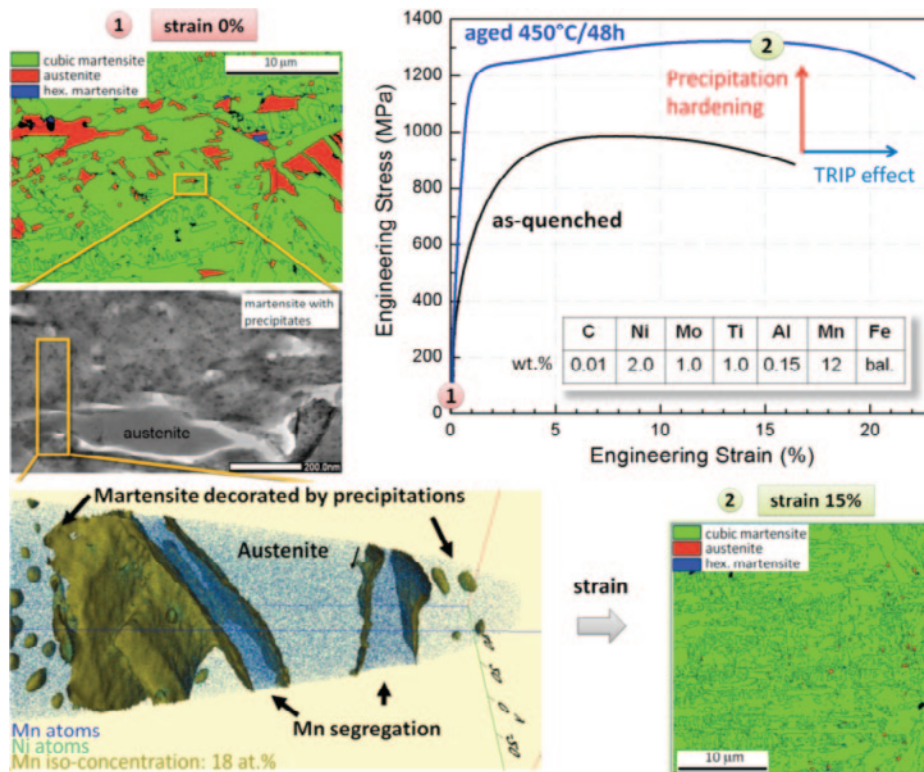
Figure 1: The stress-strain curves illustrate the increase in strength from precipitation hardening and ductility enhancement from the TRIP effect. At 0% strain (1), the electron backscatter (EBSD) phase map shows significant amounts of retained austenite. Upon 15% straining (2), the retained austenite disappears in an EBSD phase map taken at the same magnification. The APT analysis shows nanoparticles inside the martensite matrix and precipitate-free austenite regions. The Mn-enriched layers (up to 27 at.%) at the interfaces between austenite and martensite are due to partitioning, subsequent austenite reversion, and kinetic freezing of Mn in the interface region [2].

to carbide precipitation in steels, the existence of such GP zones during the early stages of precipitation of nitrides had never been reported [5].

Whereas niobium nitrides and carbides can adopt the same crystallographic structure with similar lattice parameters and orientation with respect to the ferrite matrix, their nucleation mechanisms appear fundamentally different. According to their structural similarities, it would seem natural that they would adopt the same nucleation regime, which is obviously not the case. As the diffusion of solute species and the elastic strain effect cannot be directly invoked, the interfacial energy most likely plays a fundamental role in the nucleation stage. Ab-initio-type modeling is expected to bring new understanding of this difference in the nucleation mechanisms of carbonitrides and nitrides [7].

This difference in nucleation mechanisms leads to a more homogeneous spatial dispersion of particles in N-bearing steels, which has a potential for significant improvement of the mechanical response of the steel under external stress. In particular, the development of nitrogen steels, where nitrogen replaces carbon, partly or totally, could take advantage of this homogeneous distribution of nanometer-scale fully coherent nitrides [8].

Nuclear Materials

Designing novel steels also requires understanding their long-term microstructural stability and their response to external constraints (heat, deformation, radiation, oxidation, and so on). In the specific cases of nuclear reactor steels, APT has significantly contributed to the understanding of radiation effects, in terms of the formation of hardening phases and chemical changes at grain boundaries caused by radiation-induced segregation.

Within the life-extension programs developed for existing fission nuclear reactors, the microstructural evolution of ferritic steels under long-term irradiation is fairly well understood. APT has provided unique insights into the formation and nature of deleterious Cu precipitation in reactor pressure-vessel (RPV) steel welds, (Ni,Mn,Si) clustering, and late-blooming phases that contribute to the irradiation-induced hardening of these steels [9]. More recently, attention has been drawn to high-Cr ferritic/martensitic steels as structural and cladding materials in Gen IV reactors. These provide improved swelling resistance while offering promising mechanical properties. Microstructural stability under service conditions is again a major concern, particularly for the high-dose exposure expected in some Gen IV reactor designs.
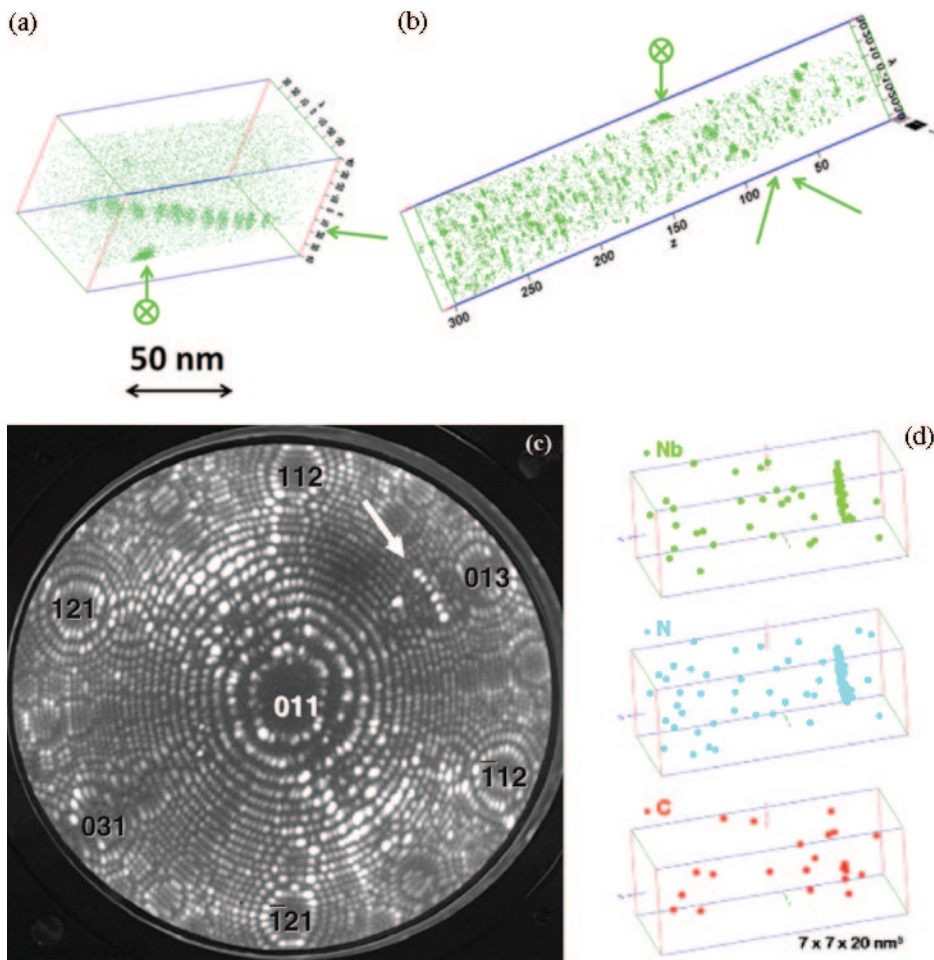
simply from observations of TEM thin foils where a few precipitates appear isolated in the matrix, APT confirms that all precipitation is heterogeneous, as not one single precipitate was detected to be isolated in the matrix. This illustrates the significant advantage of APT 3D imaging over the 2D projected TEM image obtained from a thin slice of material.

The thermal behavior of a similar alloy, where carbon was replaced by the same amount of nitrogen, was also investigated by APT. A typical 3D reconstruction is shown Figure 2b. As in the previous C-bearing sample, niobium and nitrogen precipitate together to form niobium nitrides. However, unlike the previous alloy, the distribution of particles is more homogeneous. Still, some of the largest particles are aligned along specific directions, which again is a sign of heterogeneous precipitation on dislocations. However, in this N-containing alloy, the vast majority (more than 85%) of the precipitates is homogeneously distributed in the ferritic matrix. Contrary to what was observed in the C-bearing material, precipitation of niobium nitrides in ferrite is, by nature, mainly homogeneous [4].

The early stage of nucleation of niobium nitrides was investigated at the atomic scale, using field ion microscopy and high-resolution transmission electron microscopy (HREM). The NbN nuclei form as monolayered platelets, isostructural to the parent ferritic matrix, as shown in Figures 2c and 2d. By analogy with metastable precipitates formed in aluminum-based alloys, these nuclei were called Guinier Preston (GP) zones. Despite the significant number of past studies related

Figure 2: Distribution of niobium atoms (green dots) in (a) FeNbC and (b) FeNbN alloys. Green arrows and circled crosses indicate precipitate alignments along dislocation lines, the latter being oriented normal to the figure plan. Below, analysis of an oxide dispersion strengthened ferritic steel fabricated by powder metallurgy: (c) Mn segregation to dislocations after ion implantation. (d) 3D reconstructions from powder (upper) and consolidated materials (lower). From [6].

steels can also exhibit radiation-induced segregation and precipitation. As an example, Figure 3B shows Mn segregation observed in a region free of oxide particles in an ODS steel after ion implantation [13].

Radiation damage is only one aspect of degradation taking place in nuclear reactor materials. Oxidation behavior in stainless steels exposed to nuclear reactor cooling water is another extremely important factor to understand, if the mechanisms of degradation are to be properly mitigated [14]. Until now, high-resolution oxide characterization had been achieved by analytical transmission electron microscopy (ATEM) [15]. ATEM, although very powerful, always produces results integrated over the thickness of the sample, making the observation of individual oxidized defects, such as dislocations, very challenging. It is also incapable of revealing the location of important trace elements, such as boron or lithium.

In the last few years, APT has proved to be a technique that can overcome the above-mentioned limitations. As demonstrated by Lozano-Perez and co-workers in [16], APT samples containing real surface oxides from samples exposed to nuclear reactor simulated environments can be systematically prepared with a suitable focused ion beam (FIB) instrument. This has permitted the analysis of individually oxidized grain boundaries, as well as deformation bands and dislocations in cold-worked stainless steels. In addition, lithium incorporation in the growing oxides can now be accurately quantified. Figure 4a shows a portion
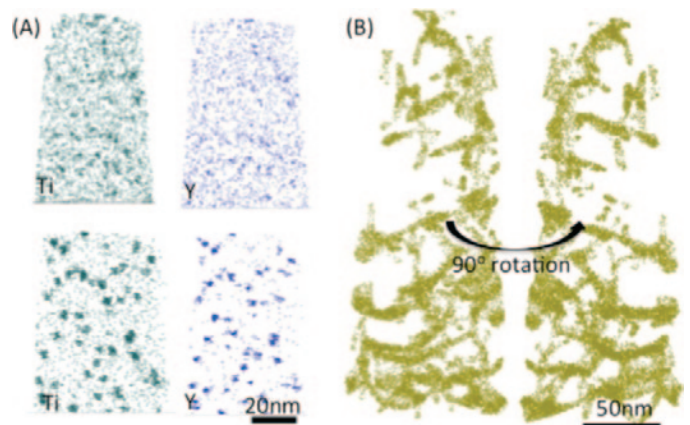
Nanostructured alloys, and oxide dispersion strengthened steels in particular, offer significant promise in terms of defect management and associated increased radiation resistance thanks to high sink densities. Because of the very small length scale associated with the nanoscale oxide distribution created during mechanical alloying, APT has naturally contributed to our understanding of these ODS microstructures. The formation of the oxide particles during consolidation has not been fully explained. Still, it is an important step toward understanding the processing/microstructure relationships needed to control the particle distribution. Although an earlier study using SANS claimed the complete dissolution of the Y_2O_3 phase [10], APT analyses revealed the existence of nanoscale clusters in milled powders [11]. Figure 3A compares the distribution of Y and Ti in ball-milled powder and hot-isostatically pressed material. The presence of a nanoscale dispersion of oxide particles and the associated high density of interfaces has been shown to be beneficial for swelling resistance and resistance to large cavity formation at grain boundaries [12]. The behavior of the particles themselves during irradiation is unclear and appears to depend on radiation conditions. Additionally, similarly to austenitic steels, ODS

Figure 3: Analysis of an oxide dispersion strengthened ferritic steel fabricated by powder metallurgy. (A) Mn segregation to dislocations after ion implantation. (B) 3D reconstructions from powder (upper) and consolidated materials (lower).
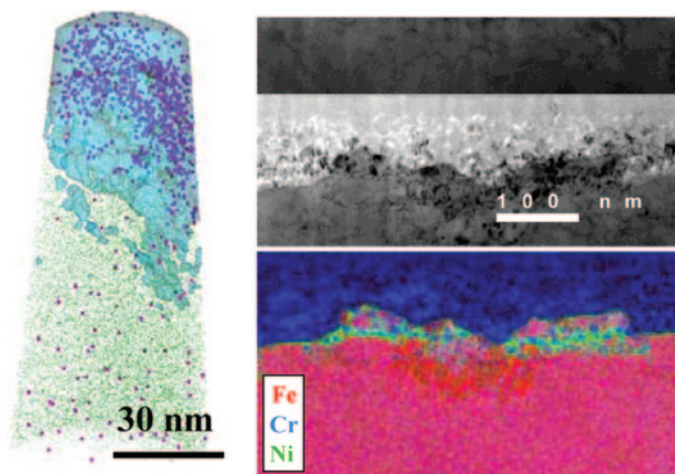
Figure 4: APT 3D reconstruction showing the surface oxides in a 304SS exposed to PWR primary water (left), where Cr-rich oxides are shown as a volume containing >10at.% O (semi-transparent light blue), Ni atoms (green) and Li atoms (red). TEM bright field cross-sectional view of the same sample showing the Cr-rich surface oxide (top right), and red-green-blue composition (Fe [red], Cr [blue] and Ni [green]) EFTEM (energy-filtered TEM) elemental maps from the same region (bottom right).

of the internal Cr-rich oxide grown in a 304SS exposed to simulated primary pressurized water reactor (PWR) water for 1500 h. The APT reconstruction shows a Cr-rich oxide as a semi-transparent volume containing >10%at. O, with oxidized dislocations extending beyond the "bulk" surface, and the location of the incorporated Li atoms (shown as red). The same region was also characterized by ATEM (Figure 4b) to reveal the location of oxidized dislocations in projection. These observations shed new light on the role of defects and applied stress on oxidation, which helps in understanding complex stress corrosion cracking (SCC) mechanisms.

Conclusion

This article illustrates how the use of APT in combination with mechanical property measurements, and processing conditions (controlled irradiation or corrosive testing), can advance our understanding of structural materials and steels in particular. By providing reliable and insightful knowledge about behavior under thermal, mechanical, and in-service conditions, new processing-structure-property relationships can be developed for designing higher-performance materials.

References

[1] M De Meyer, D Vanderschueren, and BC De Cooman, *ISIJ Int* 39 (1999) 813–22.
[2] O Dmitrieva, D Ponge, G Inden, J Millán, P Choi, J Sietsma, and D Raabe, *Acta Mater* 59 (2011) 364–74.
[3] E Courtois, T Epicier, and C Scott, *Micron* 37 (2006) 492–502.
[4] A Deschamps, F Danoix, F De Geuser, T Epicier, H Leitner, and M Perez, *Mater Lett* 65 (2011) 2265–68.
[5] F Danoix, E Bémont, P Maugis, and D Blavette, *Advanced Engineering Materials* 8 (2006) 1202–05.
[6] F Danoix, T Epicier, F Vurpillot, and D Blavette, *J Mater Sci* 47 (2012) 1567–71.
[7] D Tingaud and P Maugis, *Comp Mater Sci* 49 (2010) 60–63.
[8] XC Xiong, A Redjaïmia, and M Gouné, *Scripta Mater* 63 (2010) 1232–35.
[9] GR Odette and RK Nanstad, *JOM* 61(7) (2009) 17–23.
[10] M Ratti, D Leuvrey, MH Mathon, and Y de Carlan, *J Nucl Mater* 286 (2009) 540–43.
[11] M Brocq, B Radiguet, JM Le Breton, F Cuvilly, P Pareige, and F Legendre, *Acta Mater* 58 (2010) 1806–14.
[12] GR Odette, MJ Alinger, and B Wirth, *Annual Review of Materials Research* 38 (2008) 471–503.
[13] CA Williams, J Hyde, GDWS Smith, and EA Marquis, *Scripta Mater* 412 (2011) 100–05.
[14] RW Staehle in *Proceedings of the 15th International Conference on Environmental Degradation*, ed. Busby JT et al., TMS, Colorado Springs, 2011, 1535–1625.
[15] K Arioka, T Yamada, T Terachi, and G Chiba, *Corrosion* 62 (2006) 568–75.
[16] S Lozano-Perez, DW Saxey, T Yamada, and T Terachi, *Scripta Mater* 62 (2010) 855–58.

Mᴛ